Pre-breakdown optical phenomena in solid dielectrics acted upon by coherent radiation

N. F. Pilipetskiĭ, B. I. Makshantsev, A. A. Kovalev, M. B. Agranat, A. A. Golubtsov, S. Yu. Savanin, and O. G. Stonik

Institute of Mechanics Problems, USSR Academy of Sciences
(Submitted 12 February 1979)
Zh. Eksp. Teor. Fiz. **76**, 2026–2038 (June 1978)

The phenomena of scattering of coherent radiation in a number of transparent solid dielectrics, as well as the emission produced in them under the influence of this radiation, are investigated experimentally. A theoretical explanation is offered for the observed phenomena and accounts well for the experimental data.

PACS numbers: 77.50. + p, 78.45. + h

INTRODUCTION

The many experimental and theoretical papers published to date (see, e.g., Refs. 1–6) indicate that damage in transparent solid dielectrics by laser radiation is due to absorbing micro-inclusions. These inclusions, however, are only a fraction of the ensemble of inhomogeneities present in the dielectric, and it is as yet impossible to separate them from the total bulk of the inhomogeneities.

At the same time, this is most urgent for the formulation of the requirements that must be satisfied in the technology of the production materials used in elements of high-power optics. There are as yet no methods for determining such absorbing-inclusion parameters as the size and the absorption coefficient. Knowledge of these parameters will make it possible to determine the temperature to which the inclusion is raised by the laser radiation, an important factor for the substantiation of any theoretical model of optical breakdown. Great interest attaches therefore to various research methods capable of yielding just this information.

We consider in this paper two groups of phenomena that seem to us to be most promising from this viewpoint.

First among them is nonlinear scattering of laser radiation of below-threshold power density in solid transparent dielectrics, first observed in corundum crystals by Danileĭko, Manenkov, *et al.*,[7] who detected, in particular, time oscillations of the intensity of the scattered radiation. They have suggested that these oscillations are due to scattering of the incident radiation by the thermal fields produced when the absorbing inhomogeneities are heated.

The explanation proposed in Refs. 7 and 8 for these oscillations is based on consideration of the heating of an individual absorbing inclusion and on introduction of a steplike boundary of the temperature front at a distance $r \sim \sqrt{\chi t}$, where χ is the thermal diffusivity and t is the time of action of the radiation. In Refs. 7 and 8 the presence of this boundary was attributed to the finite propagation velocity of the temperature front at $r \sim \sqrt{\chi t}$. The influence of the finite heat propagation velocity affects the distance $r \sim St$ (S is the speed of sound in the medium).[9] Inasmuch as in the region $r \sim St$ the temperature hardly differs from the initial sample temperature, allowance for the finite heat propagation velocity leads only to corrections in the intensity of the scattered radiation, of the order of $k^2\chi^2/S^2 \sim 10^{-5}$. Here $k = 2\pi n/\lambda$, λ is the wavelength of the radiation in vacuum, and n is the refractive index of the medium.

Makshantsev and Kovalev,[10] whose work is in effect an extension of Refs. 7 and 8, have shown that all the difficulties in the explanation of the experimental relations obtained in Ref. 7 are eliminated if it is assumed that the absorbing inhomogeneities in the corundum crystal are heated to temperatures higher than the melting temperature T_{melt}. This justifies physically the existence of an interface between the liquid and solid phase, moving with a velocity $\sim\sqrt{\chi t}$, in which the dependence of the refractive index n on the temperature T can be a nonmonotonic discontinuous function or have a discontinuous derivative $\partial n/\partial T$. In all these cases the intensity of the scattered radiation can oscillate in time.

In this paper we attempt to demonstrate the feasibility in principle of using nonlinear scattering by absorbing inclusions to determine their parameters. We have developed for this purpose a procedure that is new compared with that of Ref. 7 and makes is possible to obtain the scattering from the individual largest absorbing inhomogeneities.

We calculate within the framework of the physical model proposed in Ref. 10 the shape of the scattered-radiation pulse for different values of the inhomogenity radius a, its absorption coefficient $\varkappa$, and refractive index n_a. The corresponding values of a, $\varkappa$, and n_a are determined by means of a best fit of the theoretical and experimental relations.

Another phenomenon with which one can hope to obtain additional information on the properties of the absorbing inclusions is the subthreshold emission observed in Refs. 11 and 12. We have investigated the spectrum of this emission produced by applying to a dielectric a laser single pulse of duration 4×10^{-8} sec. A theoretical interpretation of the experimental data is proposed. One can expect a thorough study of the spectra of the subthreshold emission will yield additional independent information on the parameters of the absorbing inclusions. In particular, it will make it possible to determine the temperature to which the absorbing inhomogeneities are heated under the influence of laser radiation.

 0038-5646/79/061027-06$02.40

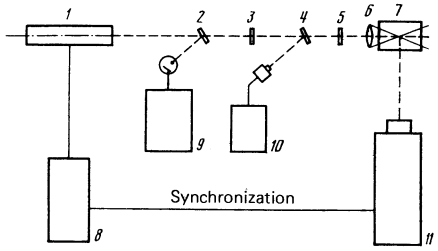

FIG. 1. Block diagram of setup for the investigation of the scattering: 1—laser with EOQS, 2 and 4—beam splitting plates, 3 and 5—light filters, 6—lens, 7—sample, 8—power supply for laser shutter, 9—oscilloscope with photoreceiver of the FÉK-09 type, 10—energy meter with head, 11—FÉR-2 streak camera.

EXPERIMENT

1. Scattering

Danileĭko *et al.*[7] used a photomultiplier (PM) to record the scattered radiation. It is quite difficult, however, to obtain from the PM information on the light scattering by a single inhomogeneity that had been visually selected beforehand with a microscope. The reason is that in the vicinity of this inhomogeneity, on which the microscope was focused, there can be situated also reversible scattering inhomogeneities not observed in the microscope before and after the irradiation, but heated by the irradiation and therefore taking part in the light scattering.

The task of our experiment is to study the dynamics of the scattering from individual absorbing inhomogeneities. This calls for obtaining not only the temporal but also spatial resolution of the scattering inclusions.

A ruby laser system was used. Its principal elements were a laser with electro-optical Q switching (EOQS) of the resonator and a streak camera (FÉR-2). The scattered radiation was received by the FÉR-2.

The laser pulses were ~60 nsec long (at the base) and had a maximum energy ~0.4 J at the emission wavelength $\lambda = 6943$ Å. The choice of active Q-switching was dictated by the need for synchronizing the operation of the pulsed units of the system (Fig. 1). The radiation

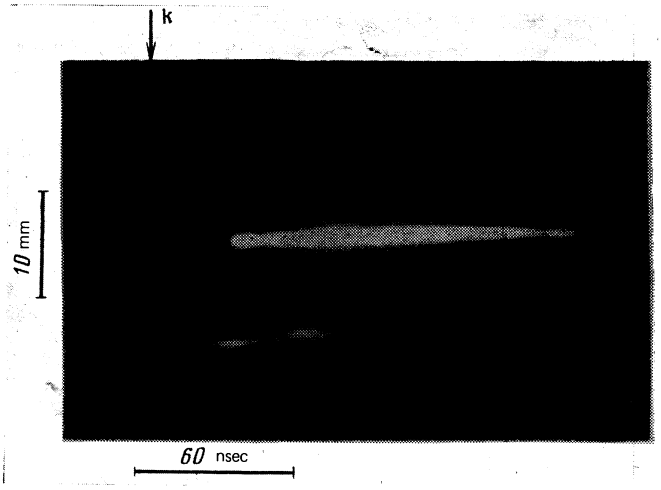

FIG. 2. Streak photograph of scattering inhomogeneities in K-8 glass.

was focused by lens 6 of focal length $F = 5$ cm onto the investigated sample 7. The energy was varied by light filters 3 and 5, and was measured with IMO-2 instrument 10. The pulse waveform was monitored by an S1-11 high-speed oscilloscope 9. The streak camera was focused on the interior of the sample in the region of the caustic of the lens 6.

The time scan of the FÉR-2 streak camera was oriented perpendicular to the radiation direction, so that the separately encountered scattering inhomogeneities in the caustic region were spatially resolved. The polarization of the incident radiation was chosen such that the intensity of the scattering in the FÉR-2 direction was maximal.

A typical streak photograph of the scattering inhomogeneities is shown in Fig. 2. The arrow **k** indicates the propagation direction of the laser beam. The time scan is from left to right. The bright line in the center of the photograph is the emission from the produced damage. The upper and lower parts of the photograph show the scan of the scattering from the inhomogeneities that were not produced in the course of the damage (as monitored visually by a microscope with auxiliary illumination from a gas laser).

It is seen from the photograph that scattering from various inhomogeneities can start at different times. This may be the cause of the oscillations of the scattered radiation when the recording is with photoreceivers of the photomultiplier type. The lower part of the photograph shows two close inhomogeneities whose scattering-intensity maxima are separated in time, but whose spatial separation is difficult even with a streak camera. When the results were reduced, account was taken only of scattering from isolated inhomogeneities with a clear surrounding field. We have investigated the following materials: polymethylmethacrylate (PMMA) and glasses of brands K-8, BK-5, and BK-10.

Figure 3 shows the photometry curves, averaged over the film grain, along the time scan of the streak photographs of the scattering inhomogeneities; here D is the photographic density of the film (isopanchromatic, 15TT800), t is the time, q is the time-averaged power density of the incident radiation, and D_0 is the film fog and the background. The experiment has revealed the

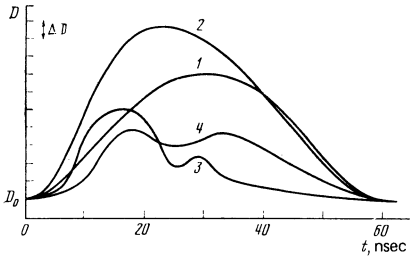

FIG. 3. Plots showing the evolution of radiation scattered by inhomogeneities in various materials: 1—subthreshold scattering typical of all materials (photographic density of film $\Delta D = 0.057$ per scale division), 2—BK-5 glass ($\Delta D = 0.0855$, $q \approx 10^7$ W/cm^2), 3—PMMA ($\Delta D = 0.057$, $q \approx 5 \times 10^7$ W/cm^2), 4—K-8 glass ($\Delta D = 0.057$, $q \approx 10^9$ W/cm^2).

following characteristic regularities of the light scattering:

1. On all the streak photographs, in all the investigated materials, the scattering inhomogeneities are spatially separated (from 3 to 10 inhomogeneities in the field of view, depending on the material).

2. At subthreshold powers, the overwhelming majority of the inhomogeneities scatter linearly in all the investigated materials. In this case the form of the scattered radiation (Fig. 3, curve 1) agrees in time with the waveform of the incident pulse. This is confirmed by the agreement between the form of curve 1 (appropriately recalculated to represent intensity) and the form of the pulse obtained from the screen of the S1-11 oscilloscope (see Fig. 1). This is also evidence of the linear regime of the operation of the installation.

3. On some photographs (approximately one frame in 20) it was possible to register distortion of the waveform of the scattered radiation at power densities $0.5q_{thr} \lesssim q < q_{thr}$ (see Fig. 3, curve 2).

4. Oscillations of the scattered radiation are observed in the immediate vicinity of the damage threshold in some cases (see Fig. 3, curves 3 and 4).

2. Emission

The spectrum of the emission produced in the prebreakdown stage was investigated in BK-8 silicon glass and also, as previously reported,[13] in PMMA, in radiation from a single-pulse laser of duration $\sim 4\times10^{-8}$ sec and wavelength $\lambda = 1.06$ μm. The emission spectrum was measured by a photoelectric procedure. The spectral lines were separated with interference filters and additional glass filters. The optical system is shown in Fig. 4.

The laser pulse is focused onto the center of the sample by a lens of focal length $F = 5$ cm. The emission produced in the focal volume was transmitted to the photoreceivers by fiber optics symmetrically located on three sides of the sample. The photoreceivers were the photomultipliers FÉU-64 and FÉU-79. The photomultiplier current pulses were recorded with the aid of S8-2 oscilloscopes. The pump light was cut off with infrared filters. Particular attention was paid to elimination of

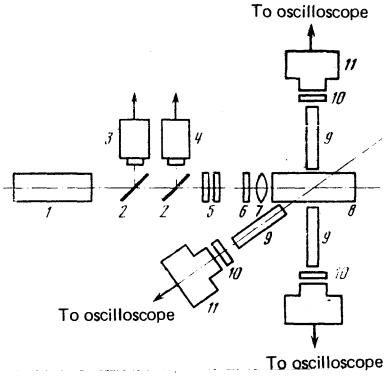

FIG. 4. Optical system of the setup for the investigation of the emission: 1—IT-181 laser, 2—beam splitting plates, 3—coaxial photocell FÉK-3, 4—calorimeters, 5—attenuators, 6—infrared filter, 7—focusing lens, 8—sample, 9—fiber optics, 10—interference light filters, 11—photomultipliers.

the background illumination, in which the principal and most appreciable interference was produced by the surface radiation due to atmospheric dust and finish defects on the sample surface. This emission is known to be produced at intensities much lower than the volume breakdown threshold.[14] A small aperture of the fiber optics or of the condenser does not eliminate this noise, since the sample acts as a waveguide because of the internal reflection from the lateral faces. To eliminate the influence of the surface emission, samples of maximum length ($l = 100$ mm) were used, the surfaces were finished with great care, and the lateral faces were blackened.

The preliminary tests were made by illuminating the sample with a parallel laser beam at the same surface power density as in the main experiments; no volume emission was produced inside the sample, since the power density was lower by three orders of magnitude. No signal was produced by the photomultipliers in this case.

In the course of the measurements we calibrated the transmission spectra of the interference filters and the spectral sensitivity of the photomultipliers (in units of ampere/watt). We measured the relative transmissions of the different "arms" of the optical system (waveguide + photomultiplier). The arm transmission was calibrated with gas lasers whose emission ($\lambda = 0.63$ and 0.44 μm) was focused into the center of the sample. The emission spectrum was measured at wavelengths $\lambda_{max} = 397$, 448, 535, 570, 600, and 725 at the same transmission bandwidth $\Delta\lambda = 12$ nm.

The laser power density was $(0.1-0.5)q_{thr}$, where q is the threshold power density at which breakdown is produced by a single irradiation. The ratio of the intensities of three selected spectral bands under single and multiple irradiation of the sample has shown that when q is varied in the range $(0.1-0.5)q_{thr}$ only the intensity of the emission of each spectral line changes, but their ratio remains the same within the limits of error. This made it possible to investigate the spectrum on several (more than three) lines with the laser radiation focused in one region of the spectrum. In these measurements we varied the transmission band of only one arm of the optical system; this made it possible to compare the results of the measurements for repeated irradiations. The photomultiplier sensitivity threshold was $\sim 10^{-8}$ W.

THEORETICAL ANALYSIS AND DISCUSSION OF THE RESULTS

1. Scattering

Consider a transparent absorbing inhomogeneity of radius a located inside a glass volume. Assume for simplicity that the thermophysical characteristics of the inhomogeneity and of the surrounding dielectric are the same. The temperature field produced as a result of the heating of the inclusion by the laser radiation is given by

$$T(r,t) = \frac{\varkappa}{\tilde{c}} \int_{r' \le a} d^3r' \int_0^t dt' q(t-t') \frac{\exp\{-|\mathbf{r}-\mathbf{r}'|^2/4\chi t'\}}{(4\pi\chi t')^{3/2}}. \quad (1)$$

Here $\varkappa$ is the absorption coefficient of the inhomogeneity, $\bar{c}$ is the specific heat capacity, $q(\tau)$ is the density of the laser radiation power in the focal volume and is approximated by

$$q(\tau)=6q\tau(1-\tau)\Theta(\tau)\Theta(1-\tau),\quad q=\frac{1}{t_p}\int_0^{t_p}q(t')dt',$$

where $\tau=t/t_p$, t_p is the duration of the radiation pulse, $\Theta(x)=1$ at $x>1$ and $\Theta(x)=0$ at $x<0$; the temperature T is reckoned from the initial temperature T_0.

We consider, as was done in Ref. 10, a very simple model, assuming that the refractive index depends only on the temperature. It is known that for a number of glasses the derivative $\partial n/\partial T$ reverses sign in the vicinity of a certain temperature T_g, which under ordinary conditions is close to the annealing temperature; the reason lies in structural changes of the material when the viscosity is changed. When the characteristic heating time t_h change, the value of T_g also changes, since these times are long enough to permit a change in structure. This change can be estimated from the relation[16]

$$\nu_h\approx\nu_0\exp\left\{-\frac{E}{T_g+T_0}\right\},\qquad(2)$$

where $\nu_h=1/t_h$, ν_0 is a frequency of the order of that of the interatomic oscillations, and E is the self-diffusion activation energy.

We determine the coordinate r_g corresponding to the temperature T_g from the equation

$$T_g=T(r_g,\,t).\qquad(3)$$

To approximate the dependence of the refractive index on the temperature we use, just as in Ref. 10, the expression

$$\begin{aligned}n-n_0=&(n_a-n_1)\Theta(a-r)+\beta_2T(r,t)\Theta(r-r_g)\\&+[n_1-n_0+\beta_1(T(r,t)-T_g)]\Theta(r_g-r),\end{aligned}\qquad(4)$$

where n_a and n_1 are the refractive indices of the inclusion and of the liquid phase of the dielectric at the temperature $T=T_g+0$; $n_0=n(T=T_0)$; $\beta_1=\partial n/\partial T|_{r=r_g-0}$ and $\beta_2=\partial n/\partial T|_{r=\infty}$ are constants.

The intensity $\Delta q(t)$ of the scattered radiation is calculated, in accord with the Rayleigh–Gans theory,[17] from the equation

$$\Delta q(t)=\frac{q(t)}{(k_0n_0Rs)^2}\left|\int_0^\infty d\rho\,\rho[n(\rho,t)-n_0]\sin(2s\rho)\right|^2\Phi(\theta,\varphi)\Delta\Omega.\qquad(5)$$

Here $k_0=2\pi n_0/\lambda$; R is the distance from the scattering point to the observation point, $\rho=k_0r$; $s=\sin(\theta/2)$, $\Phi(\theta,\varphi)=\cos^2\varphi\cos^2\theta+\sin^2\varphi$, where θ and φ are the polar and azimuthal angles of the scattering direction relative to the direction of the incident plane electromagnetic wave; $\Delta\Omega$ is the solid-angle element.

The intensity $\Delta q(t)$ (5) can be represented in the form $\Delta q(t)=AQ(t)$, where A is some constant and $Q(t)$ is determined completely by the parameters

$$B=\frac{n_a-n_1}{4\beta_2T_g}(\sin z-z\cos z),\quad z=2sk_0a,\quad L=\frac{2q\varkappa a}{\bar{c}\chi T_g}.$$

The quantity measured in the experiment was not $\Delta q(t)$ itself, but the photographic density of the film

$$D(t)=C\lg\frac{Q(t)}{G}+D_0,\qquad(6)$$

where C is a constant that characterizes the sensitivity of the photographic film, and G is some parameter that characterizes the optical properties of the measuring apparatus.

The parameters of the absorbing inclusions were determined by comparing the theoretical functions $D(t)$ calculated from formula (6) and the experimental curve shown in Fig. 5. This experimental curve was obtained with BK-10 glass. Equation (6) contains, when (1) and (3)–(5) are substituted in it, four dimensionless parameters: B, z, L, and G, and these parameters must be varied to obtain best agreement with experiment.

These unknown parameters were selected in the following manner. The experimental data were used to determine the intensities ratios of the scattered radiation

$$\gamma_1=\Delta q(t_1)/\Delta q(t_2),\quad \gamma_2=\Delta q(t_1)/\Delta q(t_3),$$

where the instants of time t_1 and t_3 correspond to the maximum intensity, and t_2 to the minimum located between them. At a fixed value of z we determined by computer calculation, from Eqs. (1) and (3)–(5), the values of B and L that satisfy the given ratios γ_1 and γ_2. The value of G was determined from the condition that the theoretical and experimental values of $D(t)$ be equal at the instant t_1. We varied next the parameter z and obtained a set of theoretical curves. The calculations have shown that the quantities B, L, and G are single-valued functions of z. The curve with the best fit to the experimental $D(t)$ determines in fact the necessary value of the parameter z, and consequently the values of B, L, and G. In these calculations we used the values[15,18] $\beta_1=-5\cdot10^{-5}$ K^{-1}, $\beta_2=3.5\cdot10^{-6}$ K^{-1}, $k_0=1.42\cdot10^5$ cm^{-1}, $\chi_3=3.9\cdot10^{-3}$ cm^2/sec, $\bar{c}=1.95$ J/cm^2. $\cdot$K, $\theta=\pi/2$ $q=8\cdot10^8$ W/cm^2.

The calculation results are shown in Fig. 5 (curve 2). This curve corresponds to $\Delta n=n_a-n_1=-0.24$, $=4\cdot10^2$ cm^{-1}, $a=2.62\cdot10^{-5}$ cm and $T_m=3.2\,T_g$, where T_m is the maximum temperature reached at the center of the inclusion. Curves 3 and 4 in the same figure correspond to the same ratios γ_1 and γ_2 as above, but to different values of the parameter z, i.e., to other dimensions a($a=2.25\cdot10^{-5}$ cm and $a=3\cdot10^{-5}$ cm). It is seen that the results are quite sensitive to the value of a, and it is this which enables us to determine the dimension of the absorbing inclusions.

We now estimate with the aid of the obtained data the absolute value of the temperature T_m. Putting in (2) $E=2.3\times10^4$ K,[15] $\nu_0\approx10^{14}$ sec^{-1}, and $\nu_h\approx10^8$ sec^{-1}, we get

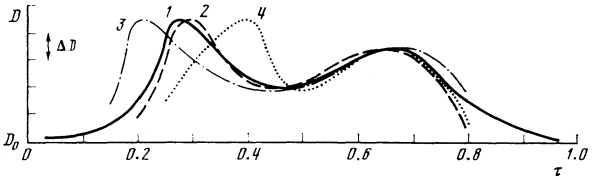

FIG. 5. Photographic density of film vs the dimensionless time τ. BK-10 glass, $\theta=\pi/2$, $\Delta D=0.057$. Curve 1—experiment, 2, 3, and 4—calculation at $z=5.25$, 4.5, and 6, respectively.

$T_m \approx 6400$ °C. So high a temperature of the absorbing inclusion, attained at subthreshold laser power, offers evidence in favor of the optical breakdown mechanism proposed in Ref. 4.

Figure 6 shows by way of illustration the theoretical dependences of Δq on the dimensionless time τ for different values of the parameter z (i.e., of the dimension a), calculated for BK-10 glass at the values of $\varkappa$ and Δn obtained above.

It should be noted that our results for the quantity $\delta = 2k_0 a|\Delta n/n_0|$ lead to $\delta \approx 1$. It is known at the same time that the Rayleigh-Gans approximation is valid only if $\delta \ll 1$. Qualitatively, however, it describes well the resonance of light also at $\delta \sim 1$. This is confirmed, for example, by the good qualitative agreement between the cross sections for the scattering by spherical particles calculated by the Mie theory[19] and in the Rayleigh-Gans approximation at values $\delta \sim 1$. In addition, the same conclusion follows for the indicated problem from a comparison of analytic results obtained by the Rayleig-Gans theory and by approximately summing the infinite series of the Mie theory.[17]

2. Emission

As shown above, the absorbing inclusions are heated in BK-10 glass at subthreshold laser power to temperatures of the order 10^4 K. It is natural to assume that the same occurs also in BK-8 glass. We can therefore attempt to interpret the experimental data shown in Fig. 7 for the dependence of the spectral emission density $J_\lambda = dI(\lambda)/d\lambda$ ($I(\lambda)$ is the intensity in a certain spectral interval) as the emission due to high-temperature heating. It follows then from our present results on scattering that we can assume this emission to be due to one strongest absorbing inhomogeneity that landed in the focal volume.

We note first of all that an analysis shows that the experimental data of Fig. 7 do not conform to radiation of Planck type, and furthermore cannot be attributed, for example to bremsstrahlung or to free-bound electronic transitions. These experimental data can be explained with the aid of bound-bound electronic transition by invoking the results of the theory of electron-vibrational transitions in emission centers[20] and in molecular objects.[21,22]

We assume for simplicity that the absorbing inhomogeneity is a crystal consisting of molecules in which only one normal mode appears spectroscopically. Next, we assume that this crystal is heated uniformly over its volume to a temperature T. Let $|f, v_f, \alpha_f\rangle$ be the states of this crystal, where f and v_f are respectively the electronic and vibrational quantum numbers, and $\alpha_f = \{n_{qs}^{(f)}\}$ is the aggregate of the phonon quantum numbers. As usual, the vibrational frequencies of the states $|v_f\rangle$ and $|\alpha_f\rangle$, $\tilde{\omega}$ and ω_{qs} are assumed to be the same in all the electronic states. Assuming that photons with wavelength λ are not absorbed in practice by the inhomogeneity, we obtain for the spectral density J of the radiation into a solid angle $\Delta\Omega$:

$$J_\lambda = \frac{64}{3}\frac{\pi^5 c^2 N a^3 \sin^2\psi \Delta\Omega}{\hbar\lambda^6} \mathrm{Av} \sum_{\substack{f'v_{f'}\alpha_{f'} \\ f>f'}} |\mathbf{d}_{f'v_{f'}\alpha_{f'}}^{fv_f\alpha_f}|^2 \delta\left(E_{fv_f\alpha_f} - E_{f'v_{f'}\alpha_{f'}} - \frac{2\pi c}{\lambda}\right). \tag{7}$$

Here N is the density of the particles in the inhomogeneity, a is its dimension, c is the speed of light, $\mathbf{d}$ is the dipole moment of the transition, and ψ is the angle between the polarization vector of the electromagnetic wave and the direction perpendicular to the dipole-moment vector of the transition. The symbol Av stands for averaging over the states f, v_f, and α_f with a distribution function $(g_f/Z)\exp\{-E_{fv_f\alpha_f}/T\}$, where g_f is the statistical weight,

$$Z = \sum_{fv_f\alpha_f} g_f \exp(-E_{fv_f\alpha_f}/T),$$

$$E_{fv_f\alpha_f} = E_f + \tilde{\omega}(v_f + {}^1/_2) + \sum_{qs} \omega_{qs}(n_{qs} + {}^1/_2).$$

The energy and temperature are expressed here in sec^{-1}.

The value of J_λ was calculated in the Condon approximation with allowance for the fact that the electronic transition takes place only between adjacent electron terms.[1)]

Recognizing that the temperature $T \sim 10^4$ K and consequently $\omega_{qs}/T \ll 1$, we can assume that

$$\frac{b_f^2}{\omega_0^2} = \frac{T}{\omega_0}\sum_{qs}\frac{\omega_{qs}}{\omega_0}(\xi_{qs}^{(f)})^2 \gg 1. \tag{8}$$

Here ω_0 is the maximum phonon frequency, particularly in the case of acoustic oscillations we have $\omega_0 = \omega_D$ (ω_D is the Debye frequency); $\xi_{qs}^{(f)}$ is the shift of the equilibrium position of the potential curve of the electronic term f relative to the term $f-1$ for normal oscillation with quasimomentum $\mathbf{q}$ and polarization s. It is known[20] that the inequality (8) in the theory of the spectra of absorption by impurity centers in a crystal corresponds to strong electron-phonon coupling. Two limiting cases are then possible.

The first case corresponds to the situation when the Franck-Condon factor for the intramolecular normal oscillation that appears in the spectrum is $F_{v_f v_{f-1}} \propto \delta_{v_f v_{f-1}}$, where $\delta_{v_f v_{f-1}}$ is the Kronecker symbol. However, a comparison of the result that follows from (1) in this case with the experimental data shows that this possibility is not realized, since the absolute value of J_λ turns out to be much lower than the sensitivity threshold of the employed apparatus. The experimental curves

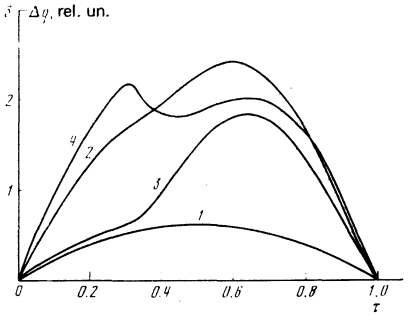

FIG. 6. Theoretical dependences of the intensity of the scattered radiation Δq on the dimensionless time τ. BK-10 glass, $\theta = \pi/2$, $q = 8\times10^8$ W/cm^2. Curves 1, 2, 3, and 4 correspond respectively to the values $z = 2$ ($T_m = 0.97\ T_g$), 3 ($T_m = 1.76\ T_g$), 4 ($T_m = 2.49\ T_g$) and 5.25 ($T_m = 3.2\ T_g$).

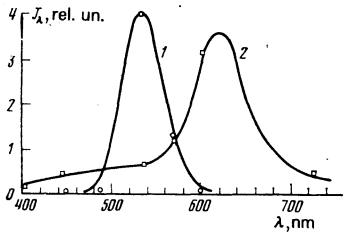

FIG. 7. Emission spectrum. Experimental points: ○—BK-8 glass, □—PMMA; calculated curves: 1—BK-8 glass, 2—PMMA.

can be attributed only to the other limiting possibility, when in addition to (8) there is satisfied also the inequality

$$\tilde{\omega}^2/b_f^2 \gg 1. \tag{9}$$

Taking (8) and (9) into account, as well as the inequality $\tilde{\omega}/T \ll 1$, we get[20,21]

$$J_\lambda = \sum_f J_f \left(\frac{\bar{\lambda}_f}{\lambda}\right)^6 I_{p_f}\left(\frac{T}{\tilde{\omega}}\xi_f^2\right). \tag{10}$$

Here

$$J_f = \frac{1}{6\pi^{1/2}}\left(\frac{2\pi a_0}{\bar{\lambda}_f}\right)^6 \frac{c^2e^2}{a_0^4\hbar(T\omega_0)^{1/2}}\left(\frac{d_{f\,f-1}}{a_0 e}\right)^2 Na^3|\Delta\Omega|\sin^2\psi\left(\sum_{qs}\frac{\omega_{qs}(\xi_{qs}^{(f)})^2}{\omega_0}\right)^{-1/2}$$

$$\times\frac{g_f}{Z_0}\exp\left\{-\frac{E_f}{T}-T\sum_{qs}\frac{(\xi_{qs}^{(f)})^2}{\omega_{qs}}-\frac{\xi_f^2}{2}+\frac{\tilde{\omega}p_f}{2T}-\frac{T}{\tilde{\omega}}\xi_f^2\right\},$$

where $\bar{\lambda}_f = 2\pi c/(E_f - E_{f-1})$, a_0 is the Bohr radius, e is the electron charge, $d_{f\,f-1}$ is the pure electronic matrix element of the dipole moment of the transition, $Z_0 \sum_f g_f \exp(-E_f/T)$, ξ_f is the ratio of the shift of the equilibrium terms to the amplitude of the zeroth intramolecular normal oscillation

$$p_f = E\left(\frac{E_f - E_{f-1}}{\tilde{\omega}}\left|1-\frac{\bar{\lambda}_f}{\lambda}\right|\right),$$

$E(\ldots)$ is the integer part of the number, and I_{p_f} is a Bessel function of imaginary argument.

From (10) we get at $p_f\tilde{\omega}/2T \ll 1$, $p_f \gtrsim 1$, and $2(T\xi_f^2/\tilde{\omega})^2 \gtrsim p_f^2$ (Refs. 20–22):

$$J_\lambda \approx \sum_f \frac{J_f}{\pi|\xi_f|(2\pi/\tilde{\omega})^{1/2}}\left(\frac{\bar{\lambda}_f}{\lambda}\right)^6 \exp\left[-\frac{\left(\frac{\bar{\lambda}_f}{\lambda}-1\right)^2}{\Delta_f^2}\right], \tag{11}$$

where $\Delta_f^2 = 2T\tilde{\omega}\xi_f^2/(E_f - E_{f-1})^2$.

Since the experimental data show that the maximum of the emission is in the region of 2–2.5 eV, it is clear that the sum over f in (11) receives the main contribution from levels with numbers $f > 0$.

For BK-8 glass, in particular, it suffices to retain only one term with a certain number $f \neq 0$. As a result, assuming the parameters $\lambda_f = 540$ nm and $\Delta_f^2 = 3.94 \times 10^{-2}$, we have a curve that describes well the experimental data (see Fig. 7, curve 1). The data for PMMA can be explained by limiting the sum over f in (11) to two terms. Assuming the parameter values $\bar{\lambda}_{f_1} = 1200$ nm, $\bar{\lambda}_{f_2} = 628$ nm, $\Delta_{f_1}^2 = 0.88$ and $\Delta_{f_2}^2 = 4.68 \cdot 10^{-3}$, we obtain curve 2 of Fig. 7.

We now estimate the power radiated by the absorbing inhomogeneity in the interval $|\Delta\lambda| = 12$ nm, and show that a reasonable values of the parameters the quantity $J_\lambda|\Delta\lambda|$ exceeds the power sensitivity threshold $\sim 10^{-8}$ W of the employed apparatus. Assuming parameters $\omega_0 \sim 10^{13}$ sec^{-1}, $d_{f\,f-1} \sim ea_0$, $\sum_{qs}\xi_{qs}^2/\omega_{qs} \approx 2 \cdot 10^{-15}$ sec, $\tilde{\omega} \sim 10^{14}$ sec^{-1}, $E_f \approx 6 \cdot 10^{15}$ sec^{-1}, $\xi_f^2 \approx 0.2$, $N \sim 10^{23}$ cm^{-3}, $a \approx 3 \cdot 10^{-5}$ cm (see above) and $T \approx 10^{15}$ sec^{-1} (≈ 7000K), we obtain

$$J_\lambda|\Delta\lambda| \sim 10^{-7}\ \text{W}.$$

Thus, the proposed model accounts qualitatively well for the experimental results at reasonable values of the parameters ω_0, $\tilde{\omega}$, ξ_f^2, etc. However, the final answer, whether the observed emission is due to high-temperature heating of the absorbing inclusions, calls for additional research. In particular, we cannot determine from the experimental data in Fig. 7 the temperature T. This calls for an investigation of the detailed structure of the $J_\lambda(\lambda)$ curve in a larger wavelength interval [see (10)].

[1)]This situation obtains, e.g., in the hydrogen atom, where even in the quasiclassical region the transitions occur in practice only between neighboring electronic terms.

[1]P. A. Avizonis and T. Farrington, Appl. Phys. Lett. **7**, 205 (1965).
[2]Yu. K. Danileĭko, A. A. Manenkov, A. M. Prokhorov, and V. Ya. Khaimov-Mal'kov, Zh. Eksp. Teor. Fiz. **58**, 31 (1970) [Sov. Phys. JETP **31**, 18 (1970)].
[3]R. W. Hopper and D. R. Uhlman, J. Appl. Phys. **41**, 4023 (1970).
[4]S. I. Anisimov and B. I. Makshantsev, Fiz. Tverd. Tela (Leningrad) **15**, 1090 (1973) [Sov. Phys. Solid State **15**, 743 (1973)].
[5]A. A. Kovalev, B. I. Makshantsev, B. F. Mul'chenko, N. F. Pilipetskiĭ, Zh. Eksp. Teor. Fiz. **70**, 132 (1976) [Sov. Phys. JETP **43**, 69 (1976)].
[6]I. V. Aleshin, S. I. Anisimov, A. M. Bonch-Bruevich, Ya. A. Imas, and V. L. Momolov *ibid.* **70**, 1214 (1976) [**43**, 631 (1976)].
[7]Yu. K. Danileĭko, A. A. Manenkov, V. S. Nechitaĭlo, and V. Ya. Khaimov-Mal'kov, *ibid.* **59**, 1083 (1970) [**32**, 588 (1971)].
[8]Yu. K. Danileĭko, A. A. Manenkov, V. S. Nechitaĭlo, and V. Ya. Khaimov-Mal'kov, Trudy FIAN **101**, 75 (1978).
[9]P. M. Morse and H. Feshback, Methods of Theoretical Physics, Vol. 1, McGraw, 1953 [Russ. transl., Moscow, 1958, p. 803].
[10]B. I. Makshantsev and A. A. Kovalev, Pis'ma v Zh. Tekh. Fiz. **4**, 1275 (1978) [Sov. Tech. Phys. Lett. **4**, 513 (1978)].
[11]Ya. A. Imas, V. L. Mokolov, and V. S. Salyadinov, Abstracts of 3rd All-Union Conf. on the Physics of Interaction of Optical Radiation with Condensed Media, 1974, Leningrad, p. 1.
[12]A. S. Glebov, Ya. A. Imas, and V. S. Salyadinov, Abstracts of 4th All-Union Conf. on Nonresonant Interaction of Optical Radiation and Matter, Leningrad, 1978, p. 126.
[13]M. B. Agranat, R. K. Leonov, B. I. Makshantsev, and N. P. Novikov, *ibid.*, p. 7.
[14]N. Bloembergen, Appl. Optics **12**, 661 (1973).
[15]M. S. Gomel'skii, Tonkiĭ otzhig opticheskogo stekla (Fine Annealing of Optical Glass), Leningrad, 1969, pp. 27 and 41.
[16]L. A. Girifalco, Statistical Physics of Materials, Wiley, 1973.
[17]R. W. Hart and E. W. Montroll, J. Appl. Phys. 22, 376 (1951).
[18]Soviet standard GOST 13 659-68.
[19]W. J. Pangonis, W. Heller, and N. A. Econcomou, J. Chem. Phys. 34, 960 (1961).
[20]Yu. E. Perlin, Usp. Fiz. Nauk 80, 553 (1963) [Sov. Phys. Usp. **6**, 542 (1964)].
[21]L. I. Markham, Rev. Mod. Phys. **31**, 956 (1959).
[22]M. D. Frank-Kamenetskiĭ and A. V. Lukashin, Usp. Fiz. Nauk 116, 193 (1973) [**18**, 391 (1973)].

Translated by J. G. Adashko